

Annual Review of Chaos Theory, Bifurcations and Dynamical Systems
Vol. 7, (2017) 56-67, www.arctbds.com.
Copyright (c) 2017 (ARCTBDS). ISSN 2253-0371. All Rights Reserved.

Coexistence of multiple attractors, Hysteresis and Vibrational resonance in Chua's circuit driven by an Amplitude modulated force

V. Bala Shunmuga Jothi

Department of Physics, Sarah Tucker College, Tirunelveli 627 007, Tamilnadu, India.
e-mail: jjothisri@gmail.com

S. Selvaraj

Department of Physics, The M.D.T. Hindu College, Tirunelveli 627 012, Tamilnadu, India.
e-mail: zelvaraj@rediffmail.com

V. Chinnathambi

Department of Physics, Sadakathullah Appa College, Tirunelveli 627 011, Tamilnadu, India.
e-mail: vchinna2017@yahoo.in

S. Rajasekar

School of Physics, Bharathidasan University, Tiruchirapalli 620 024, Tamilnadu, India.
e-mail: rajasekar@cnd.bdu.ac.in

Abstract: We consider a single scroll Chua's circuit driven by an amplitude modulated force (AMF) with two widely different frequencies ω and Ω , where $\Omega \gg \omega$. Numerically we study the dynamics of Chua's circuit driven by an AMF for specific set of values of the parameters. We show the occurrence of coexistence of several period- T orbits, bifurcations of them, period-doubling route to chaos, quasiperiodic orbit, hysteresis and vibrational resonance phenomena. We characterize periodic, quasiperiodic and chaotic orbits, hysteresis and vibrational resonance phenomena using bifurcation diagram, phase portrait, Poincaré surface of section, trajectory and resonance plots.

Keywords: Chua's circuit, Amplitude modulated force, Coexistence of multiple attractors, Hysteresis, Vibrational resonance, Chaos.

Manuscript accepted Nov 28, 2017.

1 Introduction

In the past few decades, much progress has been made on exploring complexity of nonlinear circuits and dynamical systems. Observations of different properties such as multiple coexisting attractors, hysteresis and vibrational resonance have been studied in a number of different physical circuits and systems. Among all these systems, Chua's piecewise linear circuit has played a prominent role in the investigation of above said nonlinear dynamic phenomena [1-5]. Chua's circuit is a simple electronic circuit that exhibits classic chaos theory behavior. The ease of construction of the circuit has made it a ubiquitous real-world example of a chaotic system, leading some to declare it *a paradigm for chaos* [2]. Further, Chua's circuit can be easily realized by using a multilayer CNN (Cellular Non-linear Network) [6]. The Chua's circuit has been built and used in many laboratories as a physical source of pseudo random signals and in numerous experiments on synchronization studies, such as secure communication systems and simulations of brain dynamics. It has also been used extensively in many numerical simulations and exploited in avant-garde music compositions [7] and in the evolution of natural languages [8]. In recent years, the occurrence of different kinds of nonlinear phenomena in this circuit has been investigated experimentally, theoretically and numerically [9-15].

Multiple attractors coexisting as a typical bifurcation lead to unpredictable behaviour of trajectories and are considered as a source of unpredictability of a nonlinear system [16,17]. The coexistence of several attractors give rise to the possibility of hysteresis, that is, the possibility of jumping through the coexisting attractors in a way that is not reversible when we fix a parameter back to its original value [18]. It is present in mechanical systems [19], electromagnetism [20], Chemical kinetics [21], astrochemical cloud models [22] and nonlinear optics [23-25], where optical bistability has potential applications in high speed all-optical signal processing and all-optical computing. In a nonlinear system driven by a biharmonic force consisting of a low-and high-frequencies ω and Ω with $\Omega \gg \omega$, when the amplitude of the high-frequency is varied, the response amplitude at the low-frequency ω exhibits a resonance. This high-frequency force induced resonance is called *vibrational resonance* (VR) [26, 27]. The occurrence of VR has been studied in monostable [28], bistable [29], excitable and spatially extended systems [30]. Experimental evidences of vibrational resonances in a vertical cavity surface emitting laser [31] and in simple electronic circuits [32] have been reported. Recently, Jothimurugan et al. [33] showed the experimental evidence for VR in the Chua's circuit driven by biharmonic force and Abirami et al. [34] numerically observed the VR and ghost-vibrational resonance in a modified Chua's circuit model equation driven by a biharmonic force.

Motivated by the above considerations in the present work we wish to analyze numerically the occurrence of coexistence of multiple attractor, hysteresis and vibrational resonance phenomena in a single-scroll Chua's circuit driven by an amplitude modulated force (AMF). The text of this paper is organized as follows. In the next section, we present the forced Chua's circuit model. In section 3, the dynamics of this system is analyzed by

numerical simulations including bifurcation diagrams, routes to chaos, multiple coexisting attractors, hysteresis and vibrational resonance. Finally we summarize the results and indicate future directions.

2 Forced Chua's circuit equations and parameter values

The forced Chua's circuit is given by the following closed form dimensionless equations:

$$\begin{aligned}\dot{x} &= a(y - f(x)) + (f + 2g \cos \Omega t) \sin \omega t \\ \dot{y} &= x - y + z \\ \dot{z} &= -by\end{aligned}\tag{1}$$

where a and b are constant parameters, f is the unmodulated carrier amplitude, $2g$ is the degree of modulation, ω and Ω are the two frequencies of the force with $\Omega \gg \omega$, $f(x)$ represents the piece-wise linear function,

$$f(x) = cx + \frac{1}{2}(d - c)(|x + 1| - |x - 1|)\tag{2}$$

where c and d are constant parameters. For our numerical study, we fix the parameters at $a = 7.0$, $b = 14.286$, $c = 2/7$ and $d = -1/7$, $\omega = 3.5$, $\Omega = 10.5$ and with the initial conditions $x = 1.54$, $y = -0.3138$ and $z = -2.73$. For this set of values and without the external force, the circuit exhibits a chaotic single-scroll attractor. Recently Ravichandran et al. [35] studied the effect of AMF on horseshoe chaos and routes to asymptotic chaos in Duffing oscillator and Yang et al. [36] investigated the controlling VR in a delayed multistable system driven by an AMF.

3 Dynamical behaviours of the system

In this section we analyze the dynamical behaviours such as the coexistence of multiple attractors, hysteresis and vibrational resonance phenomena in the system (Eq.(1)). These behaviours are analyzed by varying the amplitudes and frequencies of the force.

3.1 Coexistence of multiple attractors

As we know, a bifurcation diagram provides a global picture of different types of motions excited in association with the bifurcation parameter. For a range of f and g the system (Eq.(1)) has coexistence of several attractors. When the control parameter f or g is varied in the system (Eq.(1)) underwent period-doubling bifurcations leading to chaotic motions at some critical values. The bifurcation for the range of parameter $f \in [0, 5]$ with $g = 0$

(for $g = 0$, the system driven by the sinusoidal force $f \sin \omega t$) is shown in Fig.1(a). The magnification of a part of bifurcation diagram in Fig.1(a) is shown in Fig.1(b).

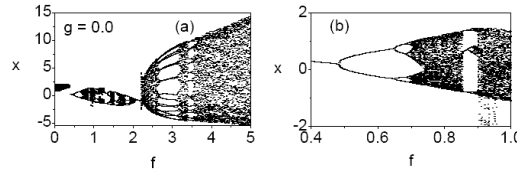


Figure 1: (a) Bifurcation diagram of Chua's circuit (Eq.(1)) under the excitation of AMF. (b) The magnification of a part of bifurcation diagram in Fig.1(a).

In this and in other bifurcation diagrams that ordinate represents the values of $x(t)$ collected at time t equal to every integral multiples of $2\pi/\omega$ (Poincaré points) after leaving the sufficient transient evolution. For $0 < f < 0.4$, a quasi-periodic is found. When f is further increased from $f = 0.4$, period-doubling, reverse period-doubling, periodic windows, chaotic motion and again quasiperiodic motion is found to occur. This is verified from phase portrait and Poincaré surface of section plot, which is presented in Fig.2. In

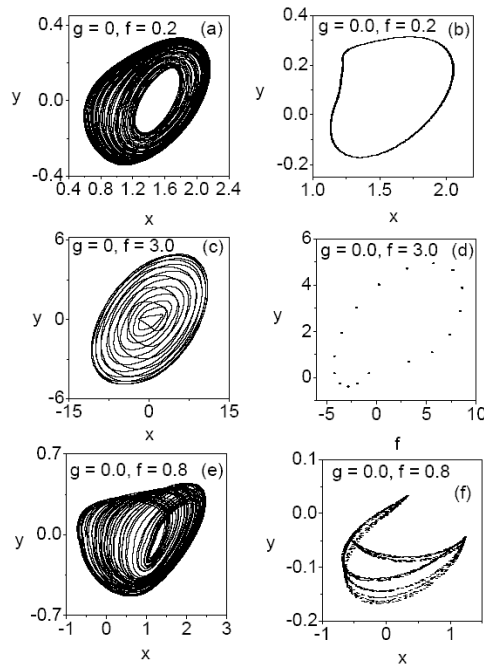


Figure 2: Phase portraits and the corresponding Poincaré maps for the system driven by an AMF for certain values of f with $g = 0$.

Fig.1(b) when f is varied from $f = 0.4$, a period- $2T$ limit cycle is developed at $f = 0.48155$. This period- $2T$ orbit becomes unstable at $f = 0.64830$ and gives birth to a limit cycle with period- $4T$. Bifurcation to a period- $8T$ orbit is observed at $f = 0.69907$. This sequence of period-doubling bifurcation accumulates at $f = 0.70723$. For $0.70723 < f < 0.85$ a chaotic motion is found. It shows the periodic motion and chaotic motion coexist for the range of $f \in [0.4, 0.85]$. When f is further increased from $f = 0.85$, again chaotic motion is found to occur. This is followed by a periodic window ($0.85 < f < 0.9$). Now we consider the effect of the AMF by fixing the value of $f = 0$ and thereby varying g , the bifurcation diagram was obtained as shown in Fig.3(a). The magnification of a part of bifurcation diagram in Fig.3(a) is shown in Fig.3(b). In Fig.3(a), we can clearly see the

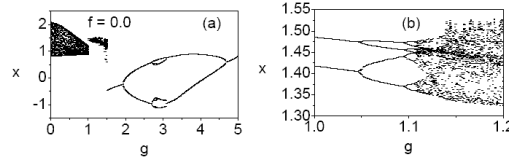


Figure 3: (a) Bifurcation diagrams of Chua's circuit (Eq.(1)) under the excitation of AMF. (b) The magnification of a part of bifurcation diagram in Fig.3(a).

occurrence of quasiperiodic, finite period-doubling, reverse period-doubling and overlap bifurcations. For $0 < g < 1$, a quasiperiodic motion is found. Overlap bifurcations is observed in the interval $1 < g < 1.2$. When g is further increased from $g = 1.2$, chaotic motion, period-doubling and reverse period-doubling is found to occur. The period- T orbit which is observed for $g > 1.5$ in Fig.3(a). This orbit is stable till g value reaches $g = 2.0$. At this critical value it becomes unstable and gives birth to period- $2T$ orbit. The newly born period- $2T$ orbit is stable up to $g = 2.65$. Bifurcation to a period- $4T$ and period- $8T$ orbits are observed at $g = 2.65$ and $g = 2.75$. When g is further increased from $g = 2.75$ a reverse period-doubling bifurcation is found to occur.

Next we show the effect of the control parameter g by fixing the values of f in a periodic region. For $f = 0.5$ and $g = 0$, the motion of the system is periodic with period- $2T$. Figure 4 is the bifurcation diagram obtained by varying g from 0 to 5. In Fig.4(a), reverse period-doubling behaviour is observed for $g \in [0, 1]$. Quasiperiodic motion is observed in the interval $1 < g < 1.7$. Figure 4(b) is the bifurcation diagram by varying g from 1.7 to 2.2. As g is increased from 1.7, the period- T orbit persists up to $g = 1.8$ and then a period- $2T$ solution is developed. This is followed by the bifurcation to $4T$ and $8T$ solutions and so on. Onset of chaos takes place at $g = g_c = 2.1225$. When the control parameter g is further increased from g_c , one finds the chaotic orbits persist up to $g = 2.5$. At $g = 2.5$ the chaotic motion disappears and the long-time motion settles to a period-doubling and reverse period-doubling behaviours.

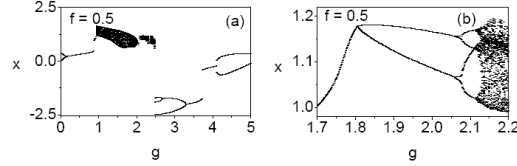


Figure 4: (a) Bifurcation diagrams of Chua's circuit (Eq.(1)) under the excitation of AMF for $f = 0.5$. (b) The magnification of a part of bifurcation diagram in Fig.4(a).

3.2 Hysteresis

First we consider the effect of low-frequency component of AMF, that is $g = 0$. When $g = 0$, the system (Eq.(1)) is driven by the sinusoidal force $f \sin \omega t$. Hysteresis is observed in the presence of $f \sin \omega t$. Bifurcation diagrams plotted by varying f in the forward direction as well as in the reverse direction is shown in Fig.5. Figure 5(a) is obtained by varying the amplitude f from a small value in the forward direction, Fig.5(b) is obtained by varying f in the reverse direction from the value 2. Different paths are followed in the Figs 5(a) and 5(b). That is the system exhibits hysteresis when the control parameter f

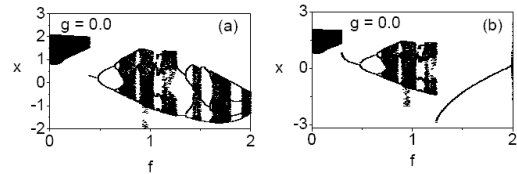


Figure 5: Bifurcation diagrams. (a) Varying the amplitude f from 0 in the forward direction (b) Varying f in the reverse direction from the value 2.

is varied smoothly from a small value to a larger one and then back to a small value.

Next we consider the system (Eq.(1)) in the presence of high-frequency component of AMF alone, that is, $f = 0$ (but $\omega \neq 0$). The amplitude of the high-frequency force is varied in the forward direction as well as reverse directions for $\omega = 3.5$ and $\Omega = 10.5$ and the bifurcation diagrams are plotted which is shown in Fig.6. Here again different path is followed when g is varied along forward and reverse directions. We can clearly notice a hysteresis in Fig.6.

Finally we consider the effect of both low and high-frequency components of AMF, that is, $f \neq 0$ and $g \neq 0$. We fix the parameters as $f = 0.5$, $\omega = 3.5$ and $\Omega = 10.5$. Hysteresis is realized when g is varied in the forward and reverse directions in the interval $g \in [0, 2]$ which is shown in Fig.7. In addition that the system (Eq.(1)) shows the period-doubling, reverse period-doubling and quasiperiodic orbits.

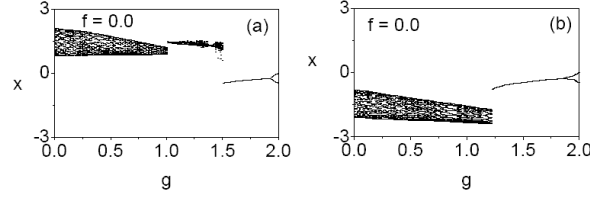


Figure 6: Bifurcation diagrams showing hysteresis phenomenon. (a) Bifurcation sequence when g is varied from 0 to 2. (b) Bifurcation sequence when g is decreased from 2 to 0.

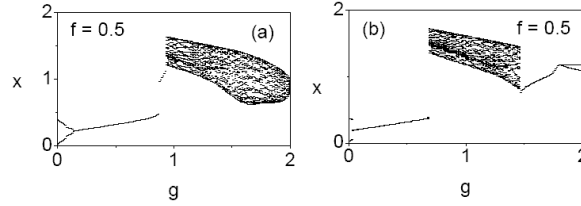


Figure 7: Bifurcation diagrams. (a) g is varied in the forward direction from 0. (b) g is varied in the reverse direction from 2.

3.3 Vibrational resonance

In addition to the coexistence of multiple attractors, hysteresis the system (Eq.(1)) exhibits also the phenomenon of VR, when g is varied. To quantify the occurrence of VR, we use the response amplitude of the system at the signal frequency ω . The system of Eq.(1) is numerically integrated using fourth order Runge-Kutta method with step size $(2\pi/\omega)/1000$. The first 10^3 drive cycles are left as transient and the values of $x(t)$ corresponding to the next 500 drive cycles are used to compute the response amplitude. From the numerical solution of $x(t)$, the response amplitude is computed through $Q = \sqrt{Q_S^2 + Q_C^2}/f$ and the phase shift $\psi = -\arctan(Q_S/Q_C)$ of the response relative to the input signal, where

$$Q_S = \frac{2}{nT} \int_0^{nT} x(t) \sin \omega t dt, \quad (3a)$$

$$Q_C = \frac{2}{nT} \int_0^{nT} x(t) \cos \omega t dt, \quad (3b)$$

where $T = (2\pi/\omega)$ is the period of the response and n is taken as 500.

Figure 8(a) shows the variation of numerically computed Q against the control parameter g . Q increases with increase in g , reaches a maximum at $g = g_{max} = 0.945$ and then decreases with further increase in g . The underlying phenomenon is VR, since the occurrence is due to high-frequency component of the force. The variation of the phase

shift ψ with the amplitude g of the high-frequency vibrational force is shown in Fig.8(b).

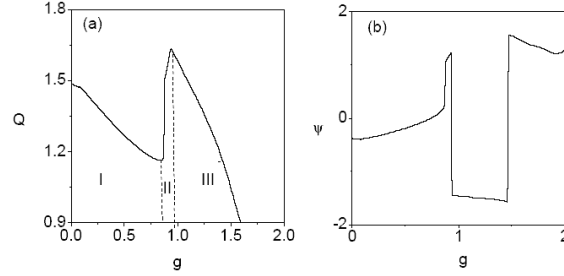


Figure 8: (a) Variation of numerically computed Q against the control parameter g . (b) The variation of phase shift ψ with the amplitude of high frequency force g .

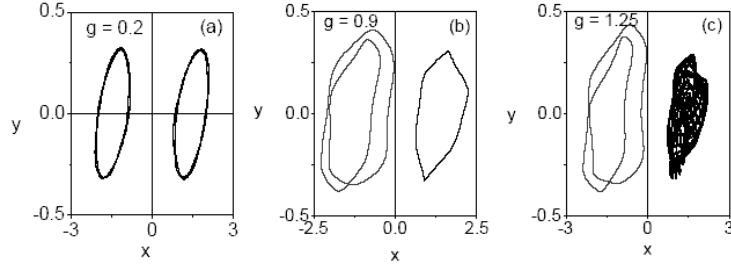


Figure 9: Phase portraits of the system (Eq.(1)) driven by an AMF for choosing the values from region-I, II, III in Fig.8.

Though the period of the orbit in the entire range of g is $T(= 2\pi/\omega)$ the response has distinct qualitative and quantitative characteristics in the regions-I, II and III. We use the tools such as phase portrait and trajectory plot to describe the dynamics in these three intervals. The phase portraits of the regions-I, II and III at $g = 0.2, 0.9$ and 1.25 are shown in Fig.9. The corresponding trajectory plot of orbits in the regions I, II and III at $g = 0.2, 0.9$ and 1.25 are shown in Fig.10.

We analyze the influence of the parameters f and ω on resonance. Figure 11 presents the results. In Fig.11(a), we observed the effect of increasing the values of ω such as $\omega = 0.1, 0.3, 0.5, 3.5$ and 7.0 and keeping the value of Ω as 10.5 , that is decreasing the ratio of Ω/ω . Resonance occurs for $\omega = 3.5$ and no resonance occurs for $\omega = 0.1, 0.3, 0.5$ and 7.0 . In Fig.11(b), $Q(g)$ is plotted for different values of f , the amplitude of low-frequency force namely $f = 0.3, 0.4, 0.5, 0.6$ with $\omega = 3.5$ and $\Omega = 10.5$. In all the cases single resonance occurs. The value of g_{max} (at which Q is a maximum) is also found to depend on f .

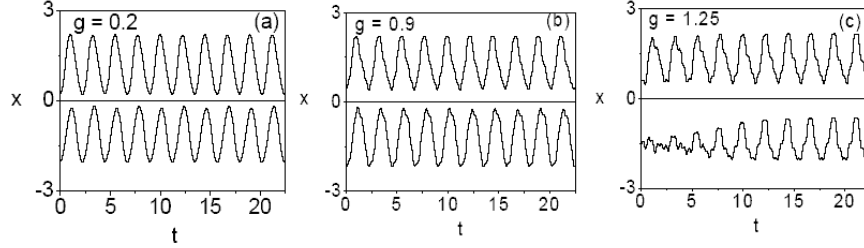


Figure 10: The trajectory plots for the three regions in Fig.8

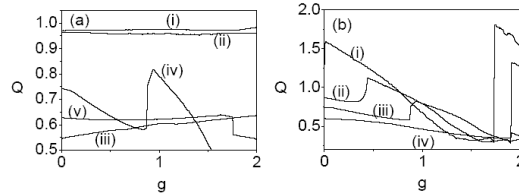


Figure 11: (a) Response amplitude Q versus g for five values of ω . The values of ω for (i), (ii), (iii), (iv) and (v) lines are 0.1, 0.3, 0.5, 3.5 and 7.0 respectively. (b) Response amplitude Q versus g for four values of f . The values of f for (i), (ii), (iii) and (iv) lines are 0.3, 0.4, 0.5 and 0.6 respectively.

4 Conclusion

In the present work, we have considered one of the most widely investigated nonlinear circuits namely the Chua's circuit which is capable of displaying a variety of complex dynamics. We numerically studied the dynamics of a single-scroll Chua's circuit driven by an AMF for specific set of values of the parameters. Coexistence of several attractors, bifurcations of them, hysteresis and vibrational resonance phenomena are encountered in the system. The system is found to be very sensitive to variations in the low-, high- and both frequency components of the AMF. We demonstrated the effect of the parameters f , g and ω on the dynamics of the system. Our study shows that bifurcations and chaotic phenomena are abundant in the Chua's circuit driven by an AMF. It is of interest to investigate certain nonlinear phenomena in the Chua's circuit driven by frequency modulated force (FMF) and experimental analysis of this circuit driven by an AMF and FMF, noise induced studies may further produce some interesting results. Work along this lines is in progress.

References

- [1] L.O. Chua, C.A. Desoer and E.S. Kuh, *Linear and nonlinear circuits*, (McGraw-Hill, Singapore, 1987).
- [2] R.N. Madan, *Chua's circuit: A paradigm for chaos* (World Scientific, Singapore, 1993).
- [3] M. Lakshmanan and K. Murali, *Chaos in nonlinear oscillators, controlling and Synchronization* (World Scientific, Singapore, 1996).
- [4] K. Murali and M. Lakshmanan, *IEEE Trans. ctkts of sys-I: Fund. Theory and Appli.*, **39(4)** (1992) 264-270.
- [5] K. Murali and M. Lakshmanan, *IEEE Trans. ctkts of sys-I : Fund. Theory and Appli.*, **40(1)** (1993) 836-840.
- [6] L.O. Chua, *Cellular Neural Networks Theory*, IEEE Transactions on Circuits and Systems. IEEE CAS, **35(10)**, (1988) 1257-1272.
- [7] E. Bilotta, S. Gervasi and P. Pantano, *Reading Complexity in Chua's Oscillator Through Music. Part I: A New Way of Understanding Chaos*, Int. J. Bifur. and Chaos, **15(2)** (2008) 253-382.
- [8] E. Bilotta and P. Pantano, *The Language of Chaos*, Int. J. Bifur. and Chaos, **16(3)** (2006) 523-557.
- [9] L. Fortuna, M. Frasca and M.G. Xibilia, *Chua's circuit implementations : Yesterday, Today and Tomorrow*, (World Scientific, Singapore, 2009).
- [10] R. Kilic, *A Practical Guide for studying Chua's circuits*, (World Scientific, Singapore, 2010).
- [11] G. Sakthivel, S. Rajasekar, K. Thamilmaran and S.K. Dana, *Statistical measures at diffusion dynamics in a modified Chua's circuit equation with multi-scroll attractor*, Int.J.Bifur. and Chaos, **22** (2012) 1250004.
- [12] S. Arathi, S. Rajasekar and J. Kurths, *Stochastic and coherence resonance in a modified Chua's circuit system with multi-scroll orbits*, Int. J. Bifur. and Chaos, **23** (2013) 1350132.
- [13] I. Gomes, M.V.D. Vermelto and M.C. Lyra, *Ghost resonance in the chaotic Chua's circuit*, Phys. Rev. E, **85** (2012) 056201.
- [14] E. Bilotta, P. Pantano and F. Stranges, *A Gallery of Chua attractors : Part I*, Int.J.Bifur. and Chaos, **17(1)** (2007) 1-60.

- [15] P. Ruiz, J.M. Guherrez and J. Guemez, *Experimental mastering of nonlinear dynamics in circuits by Sporadic pulses*, Chaos, Solitons and Fractals, **36** (2008) 635-645.
- [16] A. Ray, D. Ghosh and A. Roy Chowdhury, *Topological study of multiple coexisting attractors in a nonlinear system*, **42(138)**, Article ID. 385102, (2009).
- [17] M. Dutta, H.F. Nusse, E. Ott, J.A. Yorke and G.H. Yuan, *Multiple attractor bifurcations: a source of unpredictability in piecewise smooth system*, Phys.Rev.Letts., **83(21)** (1999) 4281-4284.
- [18] J. Borreson and S. Lynch, *Further investigation of Hysteresis in Chua's circuit*, Int. J. of bifur. and Chaos, **12(1)** (2002) 129-134.
- [19] S. Lynch and C.J. Christopher, *Limit cycles in highly nonlinear differential equations*, J. Sound Vibr., **224(3)** (1999) 505-517.
- [20] J. Szczyglowski, *Influence of eddy currents on magnetic hysteresis loops in soft magnetic materials*, J. Magn. Matter, **223(1)** (2001) 97-102.
- [21] S.K. Scott, *Oscillations, Waves and Chaos in Chemical Kinetics*, (Oxford Science Publication, 1994).
- [22] L.A.M. Nejad and R. Wagenblast, *Time dependent Chemical models of spherical dark clouds*, Astron. Astro. Phys., **350** (1999) 204-229.
- [23] A.L. Steele, S. Lynch and J.E. Hoad, *Analysis of optical bistabilities and bistability in a nonlinear optical fibre loop mirror with feedback*, Opt. Commun., **137** (1997) 136-142.
- [24] S. Lynch, A.L. Steele and J.E. Hoad, *Stability analysis of nonlinear optical resonators*, Chaos, Solitons and Fractals, **9(6)** (1996) 936-946.
- [25] S. Lynch and A.L. Steele, *Controlling chaos in nonlinear bistable optical resonators*, Chaos, Solitons and Fractals, **11(5)** (2000) 721-728.
- [26] P.S. Landa and P.V.E. McClintock, *Vibrational resonance*, J. Phys. A: Math. Gen., **33**(2000) L433-L438.
- [27] I.I. Blekhman and P.S. Landa, *Conjugate resonances and Bifurcations in nonlinear systems under biharmonic excitations*, Int. J. Nonlinear Mechanics, **39** (2004) 421-426.
- [28] S. Jeyakumari, V. Chinnathambi, S. Rajasekar and M.A.F. Sanjuan, *Single and multiple vibrational resonance in a quintic oscillator with monostable potentials*, Phys. Rev. E, **80** (2009) 046608.

- [29] S. Rajasekar, K. Abirami and M.A.F. Sanjuan, *Novel vibrational resonance in multistable system*, Chaos, **21** (2011) 033106.
- [30] E. Ullner, A. Zaikin, J. Garcia-Ojalvo, R. Bascones and J. Kurths, *Vibrational resonance and vibrational propagation in excitable systems*, Phys. Lett. A, **312** (2003) 348-354.
- [31] A.A. Zaikin, L. Lopez, J.P. Baltanos, J. Kurths and M.A.F. Sanjuan, Phys. Rev. A, **312** (2003) 348.
- [32] V.N. Chizhevsky and G. Giacomelli, *Vibrational resonance and the detection of aperiodic binary signals*, Phys. Rev. E, **77** (2008) 051126.
- [33] R. Jothimurugan, K. Thamilmaran, S. Rajasekar and M.A.F. Sanjuan, *Experimental evidence for vibrational resonance and enhanced signal transmission in Chua's circuit*, arXiv: 1308. 2463v1 [nlin.CD] 12 Aug. 2013.
- [34] K. Abirami, S. Rajasekar and M.A.F. Sanjuan, *Vibrational and Ghost vibrational resonances in a modified Chua's circuit model equation*, arXiv: 1406. 6836 v [nlin.Cd], 26 June 2014.
- [35] V. Ravichandran, V. Chinnathambi and S. Rajasekar, *Homoclinic bifurcation and chaos in Duffing oscillator driven by an amplitude modulated force*, Physica A, **376** (2007) 223-236.
- [36] J.H. Yang and X.B. Liu, *Controlling vibrational resonance in a delayed multistable system driven by an amplitude modulated signal*, Phys. Scr., **82** (2010) 025006.